A 3D REGIONAL SCALE PHOTOCHEMICAL AIR QUALITY MODEL

APPLICATION TO A 3 DAY SUMMERTIME EPISODE OVER PARIS*

A. JAECKER-VOIROL, M. LIPPHARDT, B. MARTIN, Ph. QUANDALLE and J. SALLÈS

Institut français du pétrole[1]

B. CARISSIMO, E. DUPONT, L. MUSSON-GENON and P. M. RIBOUD

Électricité de France[2]

B. AUMONT, G. BERGAMETTI, I. BEY and G. TOUPANCE

Université Paris 12 et Paris 7[3]

(1) 1 et 4, avenue de Bois-Préau,
    92852 Rueil-Malmaison Cedex - France

(2) DER,
    6, quai Watier,
    78401 Chatou Cedex - France

(3) Laboratoire interuniversitaire des systèmes atmosphériques,
    UMR CNRS 7583,
    Université Paris 12,
    61, avenue du Général de Gaulle,
    94010 Créteil - France

UN MODÈLE PHOTOCHIMIQUE 3D DE QUALITÉ DE L'AIR À L'ÉCHELLE RÉGIONALE. APPLICATION À UN ÉPISODE DE 3 JOURS À PARIS EN ÉTÉ

Cet article présente AZUR, un modèle photochimique eulérien 3D de qualité de l'air pour la simulation de la pollution de l'air dans les zones urbaines et semi-urbaines.

Ce modèle suit les évolutions des espèces polluantes gazeuses émises dans l'atmosphère par les transports routiers et les sources industrielles, il prend en compte les réactions chimiques auxquelles sont soumises ces espèces pour des conditions météorologiques en évolution (photolyse, pression, température, humidité), leur transport par le vent et leur diffusion turbulente en fonction de la stabilité de l'air. Le logiciel a une structure modulaire avec plusieurs composants dédiés à des processus spécifiques :

– MERCURE est un modèle météorologique à moyenne échelle pour déterminer les champs de vents, les coefficients de diffusion turbulente et d'autres paramètres météorologiques. C'est un modèle 3D à l'échelle régionale qui prend en compte les différentes configurations de sols et les zones de densité urbaine. Il comprend un système complet de paramètres physiques associés à des situations de ciel dégagé.

– MIEL est un modèle d'inventaire d'émissions décrivant les flux de polluants provenant des transports automobiles et des activités domestiques ou industrielles. Ce modèle comprend un inventaire des sources mobiles basé sur des comptages de véhicules sur routes associés à des informations globales sur les flux de transports déduites de données statistiques sur la population. Il utilise des facteurs d'émission spécifiques correspondant aux flottes de véhicules et à des conditions de conduites réalistes.

– MoCA est un modèle photochimique en phase gazeuse décrivant la chimie de l'ozone, des NO_x, et des composés hydrocarbonés. Ce modèle, avec 83 espèces et 191 réactions, correspond à un mécanisme réduit bien adapté à des conditions variées de qualité de l'air (allant de conditions en sites urbains à celles en sites ruraux). Pour des raisons de commodité

d'interprétation, l'identité des hydrocarbures primaires est conservée.

– AIRQUAL est un modèle eulérien 3D décrivant les phénomènes de transport par les vents et la diffusion turbulente des espèces dans l'atmosphère, il est associé à un solveur d'équations chimiques du type Gear.

Le modèle a été appliqué à un épisode estival de 3 jours au-dessus de la région parisienne. Les résultats de la simulation sont comparés aux mesures de concentrations opérées par le réseau local de surveillance (Airparif).

A 3D REGIONAL SCALE PHOTOCHEMICAL AIR QUALITY MODEL
APPLICATION TO A 3 DAY SUMMERTIME EPISODE OVER PARIS

This paper presents AZUR, a 3D Eulerian photochemical air quality model for the simulation of air pollution in urban and semi-urban areas.

The model tracks gas pollutant species emitted into the atmosphere by transportation and industrial sources, it computes the chemical reactions of these species under varying meteorological conditions (photolysis, pressure, temperature, humidity), their transport by wind and their turbulent diffusion as a function of air stability. It has a modular software structure which includes several components dedicated to specific processes:

– MERCURE, a meso-scale meteorological model to compute the wind field, turbulent diffusion coefficients, and other meteorological parameters. It is a 3D regional scale model accounting for different ground types and urban densities. It includes a complete set of physical parameterizations in clear sky.

– MIEL, an emission inventory model describing the pollutant fluxes from automotive transportation, domestic and industrial activities. This model includes a mobile source inventory based on road vehicle countings together with global information on transportation fluxes extracted from statistical population data. It uses specific emission factors representative of the vehicle fleet and real driving patterns.

– MoCA a photochemical gas phase model describing the chemistry of ozone, NO_x, and hydrocarbon compounds. This model, with 83 species and 191 reactions, is a reduced mechanism well adapted to various air quality conditions (ranging from urban to rural conditions). For interpretative reasons, the identity of primary hydrocarbons is preserved.

– AIRQUAL, a 3D Eulerian model describing the transport by mean wind flux and air turbulent diffusion of species in the atmosphere, associated with a Gear type chemical equation solver.

The model has been applied to a 3-day summertime episode over Paris area. Simulation results are compared to ground level concentration measurements performed by the local monitoring network (Airparif).

UN MODELO FOTOQUÍMICO EN 3D DE LA CALIDAD DEL AIRE A ESCALA REGIONAL.
APLICACIÓN A UN EPISODIO DE TRES DÍAS EN PARÍS, DURANTE EL VERANO

En el presente artículo se describe el AZUR, modelo fotoquímico euleriano en 3D de la calidad del aire para la simulación de la contaminación del aire en las zonas urbanas y semiurbanas.

Este modelo permite seguir las evoluciones de las especies gaseosas emitidas hacia la atmósfera por los vehículos viarios y las fuentes industriales, y tiene en cuenta las reacciones químicas a que son sometidas estas especies para condiciones meteorológicas en evolución (fotólisis, presión, temperatura, humedad), su transferencia por el viento y su difusión turbulenta en función de la estabilidad del aire. El software posee una estructura modular con varios componentes dedicados a procesos específicos.

– MERCURE es un modelo meteorológico de escala media, para determinar los campos de los vientos, los coeficientes de difusión turbulenta y, asimismo, otros parámetros meteorológicos. Se trata de un modelo en 3D a escala regional, en el que se tienen en cuenta las diversas configuraciones de suelos y las zonas de densidad urbana. También incluye un sistema completo de parámetros físicos asociados a situaciones de cielos despejados.

– MIEL es un modelo de inventario de emisiones que describe los flujos de contaminantes procedentes del tráfico rodado y de las actividades domésticas e industriales. Este modelo incluye un inventario de las fuentes móviles, que se funda en un cómputo de los vehículos en las carreteras, asociado a informaciones globales relativas a los flujos de transportes, deducidas de datos estadísticos relativos a la población. En este modelo se utilizan factores de emisión específicos que corresponden a las flotas de vehículos y a condiciones de conducción realistas.

– MoCA es un modelo fotoquímico en fase gaseosa que describe la química del ozono de los NO_x, así como de los compuestos hidrocarbonados. Este modelo, con 83 especies y 191 reacciones, corresponde a un mecanismo reducido pero perfectamente adaptado a las diversas condiciones de calidad del aire (que comienzan por condiciones en medio urbano y terminan por los emplazamientos rurales). Se ha conservado la identidad de los hidrocarburos primarios, por motivos de comodidad de interpretación.

– AIRQUAL es un modelo euleriano en 3D que describe los fenómenos de las transferencias por los vientos y la difusión turbulenta de las especies en la atmósfera, que está asociado a un sistema de resolución de ecuaciones químicas del tipo Gear.

Se ha aplicado este modelo a un episodio veraniego de tres días, por encima de la región parisiense. Se han comparado los resultados de la simulación con las mediciones de concentraciones operadas por la red local de vigilancia (Airparif).

INTRODUCTION

The study of air quality and mechanisms associated with the formation of photooxydant species, including ozone, requires the analysis of several coupled complex processes: meteorology, atmospheric chemistry, transport and turbulent diffusion of species in the atmosphere, pollutant emissions by transportation, industrial, domestic, and natural sources. Integration of these processes and their interactions requires numerical simulation.

To be manageable in terms of computer complexity, an air quality numerical model must address specific targets, defined on pertinent length and time scales. It must include a collection of homogeneous submodels solving the different physical processes at stake.

This paper describes AZUR, a numerical model simulating air quality at regional scale, in a 20 to 200 km wide and 500 m to 5 km high area above the ground, including urban, commuter belt, and rural zones, over a few days period. It is aimed at considering the influence of the different pollutant emission sources, and testing the impact of different strategies to improve air quality. These strategies include modifying the car technology, the motor fuel formulation, the energy production, or the traffic monitoring, for examples.

This model has a modular structure described in Figure 1. It includes a regional meteorological model MERCURE [1], an emission inventory model [2], the atmospheric chemical model MoCA [3], and a species transport-diffusion model associated with a Gear type chemical solver AIRQUAL.
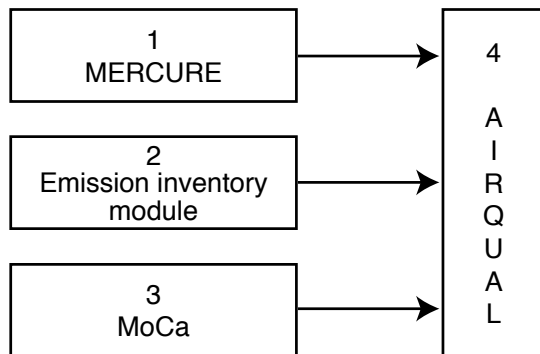

Figure 1

AZUR modular structure.

The capabilities of the model are illustrated with the simulation of a summer pollution episode over Paris.

1 GENERAL MODEL ARCHITECTURE

The mass conservation equations for reactive species transported by the mean wind flux and dispersed in the atmosphere by air turbulence are:

$$\frac{\partial c_i}{\partial t} = -\nabla(v \cdot c_i) + \nabla(K \cdot \nabla c_i) + R_i(c) + S_i - D_i(c_i)$$
$$l \leq i \leq nsp \tag{1}$$

The Equation system (1) depends on meteorological parameters. The mean wind velocity vector v and the eddy diffusivity tensor K govern transport and diffusion of chemical species in the atmosphere, while kinetics of chemical reactions depend on pressure, temperature, and humidity. The feed back influence of chemistry on meteorological parameters being neglected, meteorological calculations may be decoupled from the resolution of Equation (1). Hence, for the simulation of a specific air pollution episode, meteorological parameter values, in the simulated area and during the simulated period, are first computed with MERCURE. The emission inventory model is run separately to compute emission fluxes during the episode. The output data of these meteorological and emission simulations are then used as input data for AIRQUAL which solves the Equation system (1). This Equation system is solved numerically, after discretization with finite difference techniques on a three dimensional grid. This original Equation system is decomposed, with a fractional time step procedure, into a sequence of four elementary steps corresponding to the different contributions of pollutant emissions, transport-diffusion, chemistry, and dry deposition:

Emission sources contribution

$$\frac{\partial c_i}{\partial t} = S_i \qquad\qquad l \leq i \leq nsp \tag{2}$$

Transport-diffusion contribution

$$\frac{\partial c_i}{\partial t} = -\nabla(v c_i) + \nabla(K \nabla(v c_i)) \qquad l \leq i \leq nsp \tag{3}$$

Chemical reaction contribution

$$\frac{\partial c_i}{\partial t} = R_i(c) \qquad\qquad l \leq i \leq nsp \tag{4}$$

Dry deposition contribution

$$\frac{\partial c_i}{\partial t} = D_i(c_i) \qquad\qquad l \leq i \leq nsp \qquad (5)$$

Unlike Equation (4), emission fluxes (2), diffusion-transport (3) and dry deposition (5) are independant for each species and may be solved separately for each species.

2 METEOROLOGICAL MODEL

MERCURE is a 3D non-hydrostatic model, based on an anelastic approximation. It solves the conservation equations for mass, momentum, scalar parameters (potential temperature, specific humidity, and any passive pollutant concentration) and turbulent quantities on a staggered Arakawa-B grid. It takes the topography into account using a terrain following coordinate.

2.1 Numerics

Advection, diffusion and pressure-continuity are solved separately by a fractional time step technique:
– advection is solved with a semi-lagrangian scheme;
– diffusion uses an implicit centered finite differences scheme, solved with an alternative direction method (operator splitting in the 3 directions);
– the Poisson Equation for pressure continuity is solved with a conjugate gradient method.

The wave reflections on lateral and upper boundaries may be minimised with an absorbing layer close to the boundary where horizontal diffusion is progressively increased.

2.2 Turbulence

Two parameterizations of turbulent diffusion may be used. Both are based on the Boussinesq hypothesis, i.e. the vertical turbulent fluxes are related to the vertical gradient mean parameter values.

The first parameterization corresponds to exchange coefficients estimated with the Louis [4] and Louis et al. [5] formulation (one-order closure):

$$K_{mz} = \left|\frac{\partial V}{\partial z}\right| l^2 F_m(Ri)$$

$$\text{with } l = \frac{k_a z}{1 + \frac{k_a z}{l_{inf}}} \quad l_{inf} = 20 \text{ m} \quad (6)$$

$$K_z = \left|\frac{\partial V}{\partial z}\right| l^2 F_h(Ri)$$

F_m and F_h are two functions of the bulk Richardson number taken from [4] and [5].

The second turbulent scheme is the e-ε closure solving the conservation equation for turbulent kinetic energy and its dissipation rate (one-and-half closure). In this case diffusion coefficients are computed as:

$$K_{mz} = K_z = C_\mu \frac{e^2}{\varepsilon} \, (C_\mu = 0.09) \qquad (7)$$

2.3 Radiative effects

The shortwave radiation scheme is based on the parameterization of Lacis and Hansen [6]. Water vapor and ozone absorption and Rayleigh diffusion are parameterized in terms of integrated transmission functions. For cloudy conditions, the multiple scattering is calculated with the two-stream approximation. The cloud absorption and scattering effects are computed with the adding method.

For long-wave radiation, the radiative transfer Equation is solved with the integrated emissivity approximation. Absorptivities of Sasamori [7] are used for water vapor, water dimers, carbon dioxide and ozone. For a cloudy sky, transmission by cloud droplets is modeled with a constant absorption coefficient ($150 \text{ m}^2\text{kg}^{-1}$, according to Stephens [8]). Both schemes take the cloud fraction into account.

2.4 Surface layer

The parameterization of surface turbulent fluxes of heat, humidity, and momentum, is based on the Louis and Louis et al. formulation [4] and [5]. This formulation has the great advantage of being explicit, i.e. not requiring iterative solution techniques.

2.5 Surface processes

Two methods may be used to compute temperature and humidity surface values. With the first method, these parameter values are simply forced to values measured by the Meteo-France surface network, interpolated to model grid nodes. The second method uses a more sophisticated surface process parameterization included in MERCURE. In this case, ground surface temperature is computed according to the Deardorff force-restore model [9], using an anthropogenic heat flux. Surface humidity is calculated with a

two layers model. The local surface characteristics (roughness lengths, albedo, emissivity, etc.) are determined from a surface classification in seven categories: water, forest, bare soil, low density buildings, medium density buildings, high density buildings, and agricultural surfaces. For each type, model constants have been found in [10, 11 and 12]. The scalar roughness length has been deduced from the aerodynamical length using the following relationship [10]:

$$\ln\left(\frac{z_o}{z_{ot}}\right) = 2 \qquad (8)$$

The MERCURE model has been tested on boundary layer data (diurnal evolution during the Wangara experiment), and on orographic problems [1], by comparison with analytic solutions and with data collected during the Pyrénées experiment (PYREX). It has also been applied to simulate the land-sea breeze cycle in the framework of the APSIS project [13], and the Paris heat island met during the summer pollution episode described in this paper [14].

3 ATMOSPHERIC CHEMICAL MODEL

MoCA [3] is the atmospheric chemical model used by AZUR. It represents the complex photochemical processes involved in air quality. It simulates the formation of O_3 and other secondary pollutants, from reactions of primary species, directly emitted by the different pollution sources, under the effects of sunlight and other meteorological conditions. It has not been designed for fast computing of average pollution forecast in a particular area. It is aimed at estimating the effect of the different pollution sources, and the relevance of various possible actions on motor fuel formulation, car and industrial technologies, to improve air quality at regional scale. MoCA's objective is to accurately represent the complex effects of NO_x and VOCs on the formation of secondary pollutants as O_3. It is reliable in many different atmospheric conditions of VOC to NO_x ratio ranging from small values corresponding to urban conditions to high values characteristic of rural conditions.

MoCA has been built from a detailed atmospheric chemistry model which has been reduced using:
– the operator method proposed by Carter [15] substituting a single balance reaction to a series of several reactions associated with a VOC degradation;

– lumping of secondary VOCs into a limited number of species.

The quality of this reduction approach has been tested through comparisons with the detailed model (650 reactions, 160 species). This detailed mechanism takes into account the degradation of 12 primary VOC species covering the main chemical classes observed in real atmosphere [3]. During simulations of twelve hours long photochemical pollution periods, in a single cell reactor, differences between the two models never exceeded 3% on O_3 level and 5% on NO_x levels. This was verified for several VOC to NO_x initial ratio values ranging from five to twenty.

The set of primary species that are emitted is preserved in the MoCA model, and the reduction processes still apply to a modification of this set. This model can further be reduced for particular situations. This is the case if the VOC to NO_x ratio values are limited to high levels. It also can be upgraded with new primary emitted organic species. The addition of a new organic species in general corresponds to the addition of one species and a single per degradation mode reaction.

The MoCA equations are integrated by the chemical equation solver included in AIRQUAL. While reduced, MoCA still is a precise model with a wide range of kinetic reaction values. Its integration requires the solution of a large and stiff ordinary differential equation system. For numerical stability reasons, an implicit predictor-corrector Gear type method is necessary. AIRQUAL uses a Gear code including sparse matrix techniques, vectorized around the number of grid cells [16] and [17].

4 EMISSION INVENTORY MODEL

MIEL, the emission inventory model computes the density of pollutant fluxes emitted by all pollution sources as a function of space and time in the simulated area, and integrates these fluxes on simulation grid cells. These fluxes are the source terms S_i of Equation (2).

The emission inventory model processes all relevant informations on pollution sources in the simulated area. This data base process is managed with MapInfo, a Geographic Information System [18]. This provides to the emission inventory model a great flexibility and adaptability to treat new simulated areas with different emission conditions. To match AZUR simulation

scales, the density of pollutant fluxes must be computed with a space resolution of one square kilometer and a time resolution of one hour.

The species emissions due to transportation, industrial, domestic, and natural sources are of different nature, different magnitude, and evolve with different frequencies at simulation time scale. For these reasons, they are treated separately before being added.

Transportation has a great responsability in the air quality degradation in urban areas. 70 to 80% of NO_x and 35 to 65% of VOCs are belived to originate from transportation.

In a single day, in a regional area, the nature and magnitude of vehicle flow changes rapidly from one point to another. Reliable data on pollutant emission fluxes due to transportation requires a fine description of this traffic at proper simulation scales. A data processing method has been developped for this purpose [2].

An example of NO_x emissions, due to transportation in Paris area, as computed by the emission inventory model is described in Figure 2. Data used for emission fluxes due to industrial and domestic sources are those reported in the 1990 CITEPA study [19] using the CORINAIR approach [20].

5 TRANSPORT/DIFFUSION MODEL

5.1 Introduction

Transport/diffusion Equations (3) are independant for each species. Each equation is solved separately and numerically after discretization with finite difference schemes, on a terrain following cartesian grid. The grid spacing is variable in the vertical direction. This allows to describe ground level areas, where most pollutants are emitted, with layer thickness smaller than in higher altitude. The grid spacing is constant in horizontal directions, but it may differ from one direction to the other. Typical AZUR simulation grids cover 20 km to 200 km in horizontal directions and between 500 m to 5000 m in the vertical direction, with grid cells of 3 to 10 km wide and 25 m high near the ground to several hundred meters in altitude. Yet in general, species transport by wind dominates the diffusion associated with air turbulence in horizontal directions, while diffusion is mainly responsible for species transport in the vertical direction. Because of this discrepancies, different schemes are used to discretize diffusion and transport operators in horizontal and vertical directions.
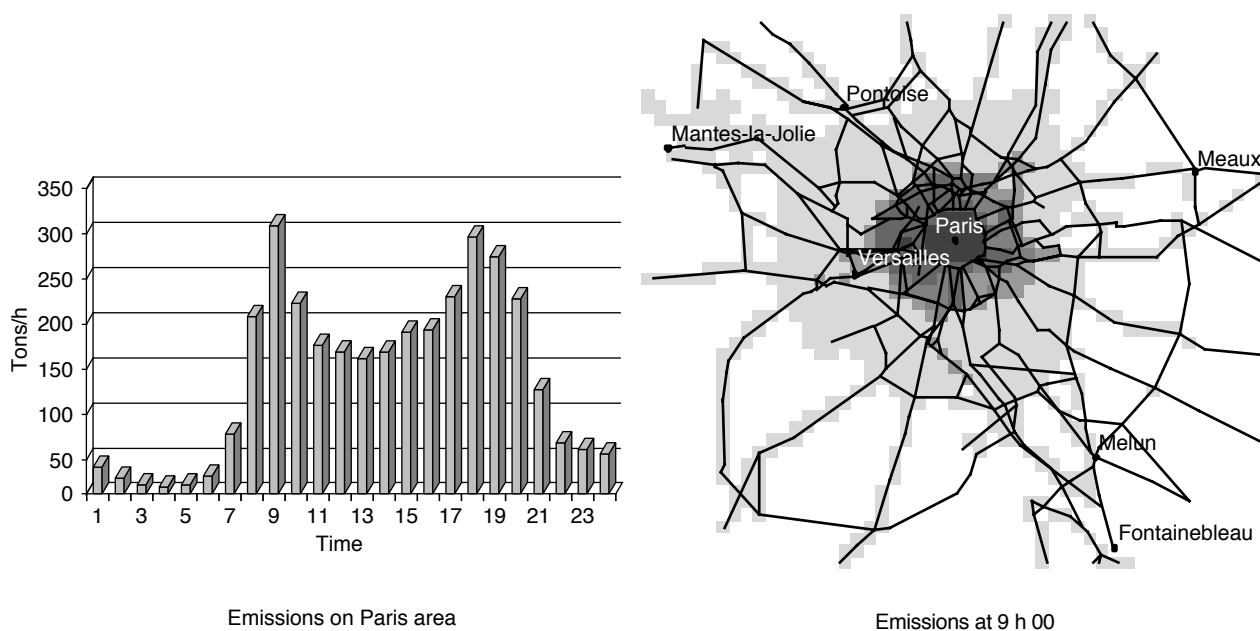

Emissions on Paris area

Emissions at 9 h 00

Figure 2

CO emissions due to tranportation in Paris area.

Still, Equation (3) is split in the three directions and solved separately for each direction.

5.2 Diffusion

In the vertical direction the diffusion operator is discretized with the following scheme adapted to variable grid spacing:

$$\frac{\partial}{\partial z}\left(K_z\,\frac{\partial c_i}{\partial z}\right) = \frac{K_{z,j\text{-}\frac{1}{2}}\dfrac{c_{i,j\text{-}1}-c_{i,j}}{\Delta z_{i\text{-}1}+\Delta z_i}+K_{z,j+\frac{1}{2}}\dfrac{c_{i,j+1}-c_{i,j}}{\Delta z_{i+1}+\Delta z_i}}{2\Delta z_i}$$

$$l \le i \le nsp \tag{9}$$

In Equation (9), cells number j-1, j, and j+1 are neighbouring cells lined up in the vertical positive direction. This scheme is conservative and first order accurate in space when grid spacing is variable. The same discretization scheme is used in horizontal directions, but in this case, it is second order accurate in space as grid spacing is constant in these directions.

A second order time implicit Crank-Nicholson scheme is used for discretization in horizontal directions:

$$\frac{\partial}{\partial x}\left(K_x\,\frac{\partial c_i}{\partial x}\right) = \frac{1}{2}\left[\left.\frac{\partial}{\partial x}\left(K_x\,\frac{\partial c_i}{\partial x}\right)\right|_n + \left.\frac{\partial}{\partial x}\left(K_x\,\frac{\partial c_i}{\partial x}\right)\right|_{n+1}\right]$$

$$l \le i \le nsp \tag{10}$$

In vertical direction, discretization steps being much smaller in general, a less precise, but numerically more stable, first order fully implicit scheme is used:

$$\frac{\partial}{\partial z}\left(K_z\,\frac{\partial c_i}{\partial z}\right) = \left.\frac{\partial}{\partial z}\left(K_z\,\frac{\partial c_i}{\partial z}\right)\right|_{n+1} \tag{11}$$

$$l \le i \le nsp$$

5.3 Transport

In each direction, the transport operator is discretized with a conservative scheme such as:

$$\frac{\partial(v_x c_i)}{\partial x} = \frac{v_{x,j+\frac{nx}{2}}.c_{i,j+\frac{nx}{2}} - v_{x,j\text{-}\frac{nx}{2}}.c_{i,j\text{-}\frac{nx}{2}}}{\Delta x} \tag{12}$$

$$l \le i \le nsp$$

In horizontal directions, species concentrations at grid cell interfaces are computed with the Ultimate Quickest scheme proposed by Leonard [21]. This upstream scheme is explicit, limited, and third order

accurate in space. It is very little dispersive and represents a good compromise between numerical stability and precision to approximate transport by wind in horizontal directions. If the x component of wind is positive, and if j-nx, j, and j+nx are the numbers of three neighbour cells lined up in the x positive direction, species concentrations at interface of grid cells j and j+nx are approximated as:

$$c_{i,j+\frac{nx}{2}} = \frac{1}{6}\left[2c_{i,j+nx} + 5c_{i,j} - c_{i,j\text{-}nx} - 3\frac{v_{x,j+\frac{nx}{2}}}{\Delta x}\left(c_{i,j+nx}-c_{i,j}\right)\right.$$

$$\left. + \left(\frac{v_{x,j+\frac{nx}{2}}}{\Delta x}\right)^2\left(c_{i,j+nx}-2c_{i,j}+c_{i,j\text{-}nx}\right)\right] \tag{13}$$

$$l \le i \le nsp$$

This face value is then submitted to a limiter based on monotony conservation.

In the vertical direction the transport operator is discretized with a more stable, first order, implicit upstream scheme:

$$c_{i,j+1/2} = c_{i,j} \qquad\qquad l \le i \le nsp \tag{14}$$

6 SIMULATION OF A SUMMERTIME POLLUTION EPISODE OVER PARIS

6.1 Introduction

AZUR has been used to simulate the air quality over Paris during the three days episode of July 29-30-31, 1992. During this episode, more than 300 μg/m³ ozone concentration levels have been measured by the Airparif local monitoring network [22].

6.2 Meteorological situation

During the entire episode, Paris region remained in a slack pressure gradient zone, leading to weak and not well organized winds near the ground. On the July 29, a SW subsidence brought very hot air associated with calm winds, leading to the formation of an exceptionally strong inversion in the evening. On July 30 at 0 h a.m., this inversion reached 11°C between 0 and 100 m, and kept this value until the end of the night. The wind speed was very weak in the morning and remained lower than 3 m/s afterwards. The screen temperature reached 35°C at its maximum. On July 31, the ground inversion amplitude was about

4°C, and the wind varied from 1 to 3 m/s. This situation was particularly favorable to the development of a high photochemical pollution: weak dispersion, high temperature, and strong insolation.

6.3 Numerical simulation

6.3.1 Introduction

The simulated area was a 120 km x 120 km square centered on central Paris. This area was covered with a 3D cartesien grid made of square grid cells of equal sizes in the horizontal plane. A 2 km grid cell resolution was used for the meteorological calculation (60 x 60 grid cells in areal directions for MERCURE simulation) while a 6 km grid cell resolution was used for the transport/diffusion/reaction calculation (20 x 20 grid cells in areal directions for AIRQUAL simulation). Interpolation of the meteorological fields were then performed from MERCURE grid nodes to get values at AIRQUAL grid nodes. This solution seemed to be a good compromise between simulation accuracy and computer time constraints.

6.3.2 Meteorology

For the MERCURE meteorological simulation, the simulation grid was extented up to 4000 m, in the vertical direction with 15 grid layers of size ranging from 20 m near the ground to 380 m at the top.

One calculation per three hours period has been performed during the three days episode. For each calculation, constant lateral boundary conditions have been derived from Trappes radiosoundings in the upper layers, and from Saclay instrumented mast in low layers. The turbulent coefficients K_{mz} and K_z were calculated with the Louis *et al.* model [5]. Surface temperature and humidity have been forced to measured values, partially corrected to take gradients between surface and measurement level (2 m) into account, assuming constant turbulent fluxes between the ground and the first grid node level.

Figure 3 shows the calculated surface wind field on July 30 at 0 h UTC, superimposed on the topography. Although topography is lower than 250 m, a strong effect of local forcing in the calculated direction exists in this case, due to the weakness of the synoptic wind and to the strong stability of air above the ground. In particular, katabatic winds may be seen in the valleys. Figure 4 presents a vertical cross-section of the

turbulent scalar diffusivity K_z on July 30 at 15 h UTC. This figure shows that depth of the mixed layer (about 1000 m) is relatively low, probably because of a large-scale subsidence.
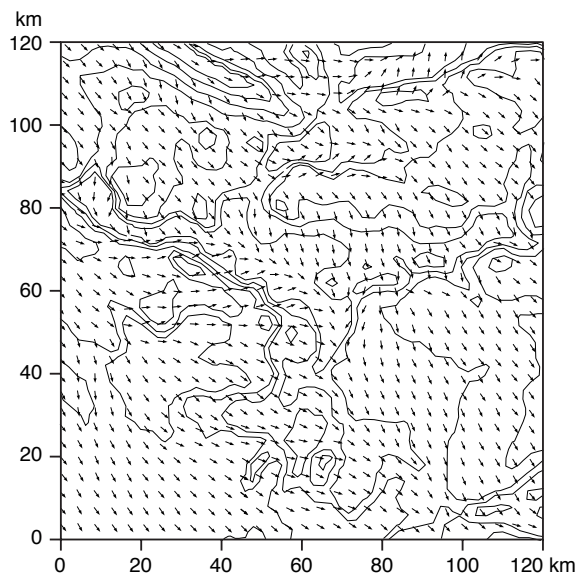

Figure 3

Surface wind simulated by the MERCURE model for July 30, 1992, at 0 h UTC. Vectors are plotted every two grid points. For the topography, the contour interval is 26 m.

6.3.3 Reactive Transport/Diffusion

For the AIRQUAL reactive transport/diffusion simulation, the vertical size of the computational domain was limited to 1500 m to cover the diffusion zone indicated in Figure 4. The grid was then limited to 10 layers in the vertical direction. The three day period was simulated with 481 transport/diffusion time steps. The simulation took 2 h of CPU time on a Fujitsu VP2400/10 vector processor, and the same simulation took 86 h on a Silicon Graphics Indy R4600 PC/133 scalar workstation.

Figure 5 to 7 show the time evolution of O_3, NO and NO_2 concentrations as calculated in the grid cell (10, 10, 1) for the three days (AZUR values in Figures 5 to 7) and as measured by three ground stations: Saint-Jacques Tower (4th Paris district), Eiffel Tower (7th district), and Health Laboratory (13th district). It should be kept in mind that the AZUR value corresponds to an average concentration calculated in a 36 km^2 arealy large and 25 m high grid cell. On the
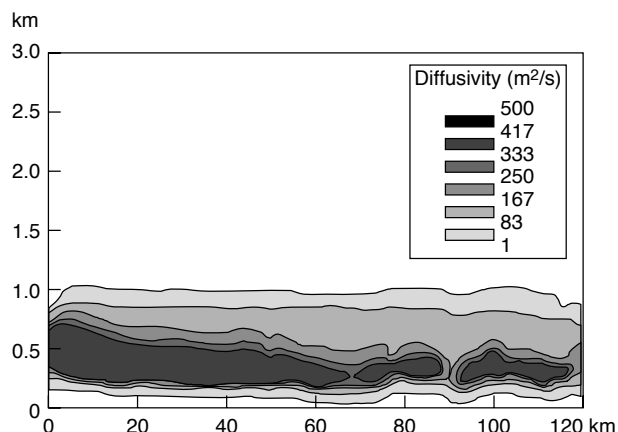
Figure 4

South-North vertical cross section (in the center of the domain) of turbulent scalar diffusivity calculated by MERCURE for July 30, 1992 at 15 h UTC.
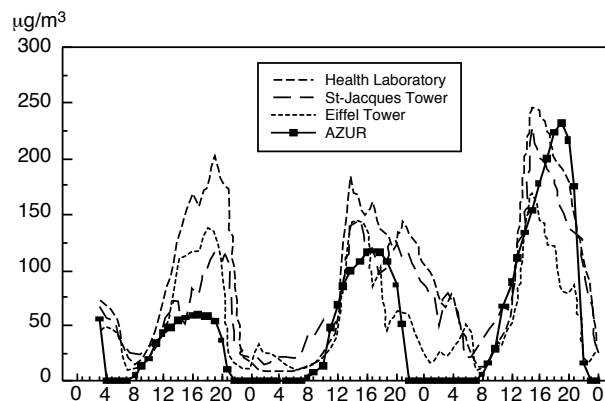

Figure 5

O_3 concentration in Paris center.

Figure 6

NO concentration in Paris center.

Figure 7

NO_2 concentration in Paris center.

contrary, the network station measurements represent the concentration at the inlet of the sampling line which is somewhat specific to the local environment. Covering of the cell area by measurements is also not homogeneous. The NW apex of the (10, 10, 1) grid cell is in the center of Paris (approximately Saint-Jacques Tower), so that the cell entirely covers the SW quadrant of Paris and extends out of Paris districts up to 2 km in SW suburbs. The Eiffel Tower station is positioned just on the north side of the grid cell, 1 km cast of the NW cell apex. Health Laboratory station is located out of the cell, about 2 km east from the center of the eastern cell side. Consequently the data available from the network are only representative of the north side of the cell and, to a less extent, of the east side. No data exist for the center, south, and west part.

Nevertheless results on O_3 (Fig. 5) indicate a good agreement between simulation data and measurements, except for July 29. This is the first simulation day and it is possible that the model is not yet stabilized and that concentrations of compounds absent from the initial condition set have not yet reached their stationary state. There is also a good agreement between simulation results and measured values for NO and NO_2 concentrations (Figs. 6 and 7). Calculated trends are in good agreement with measurements. However, large differences may be observed at certain times, for different stations. This is the case for NO on July 30. A large discrepancy exists between calculation and measurements at the Eiffel Tower station in the middle
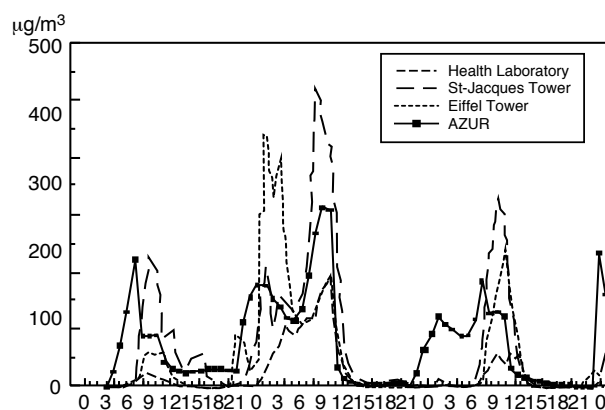
Figure 8

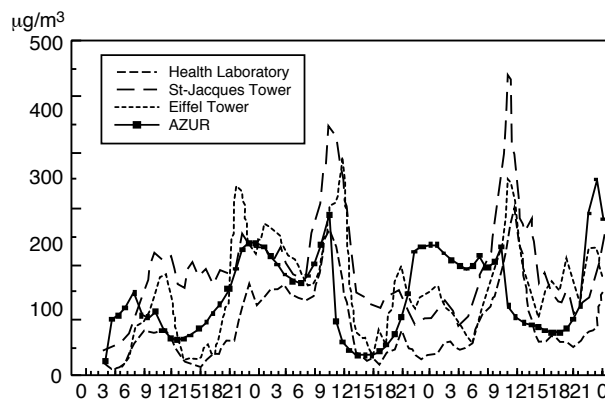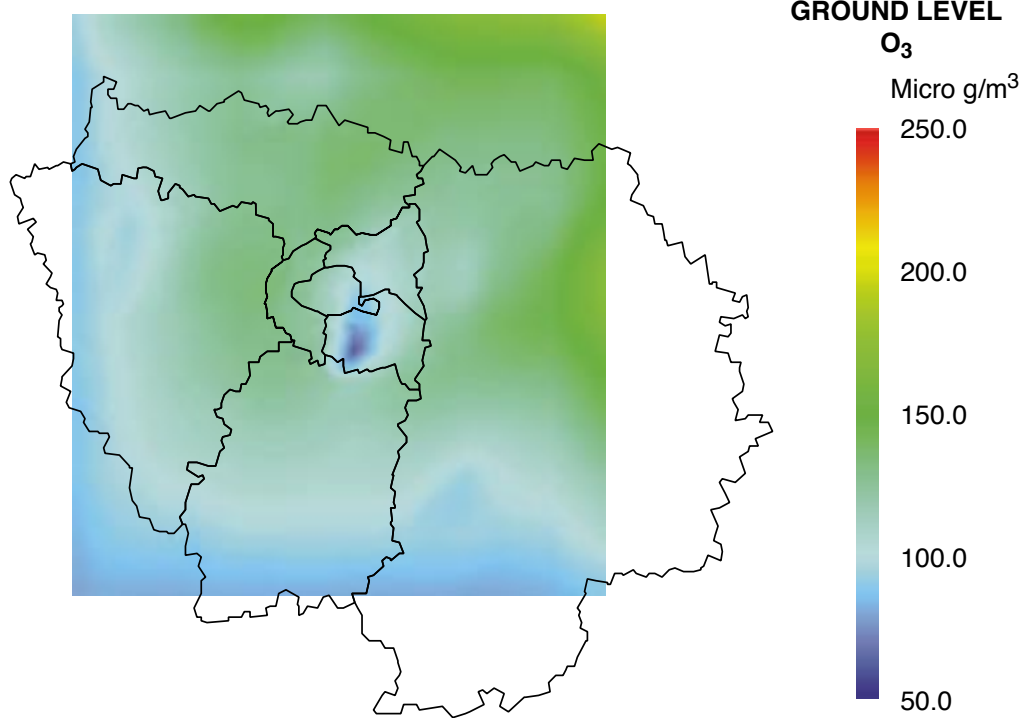O$_3$ concentration over Paris at 15 h UTC on July 30.
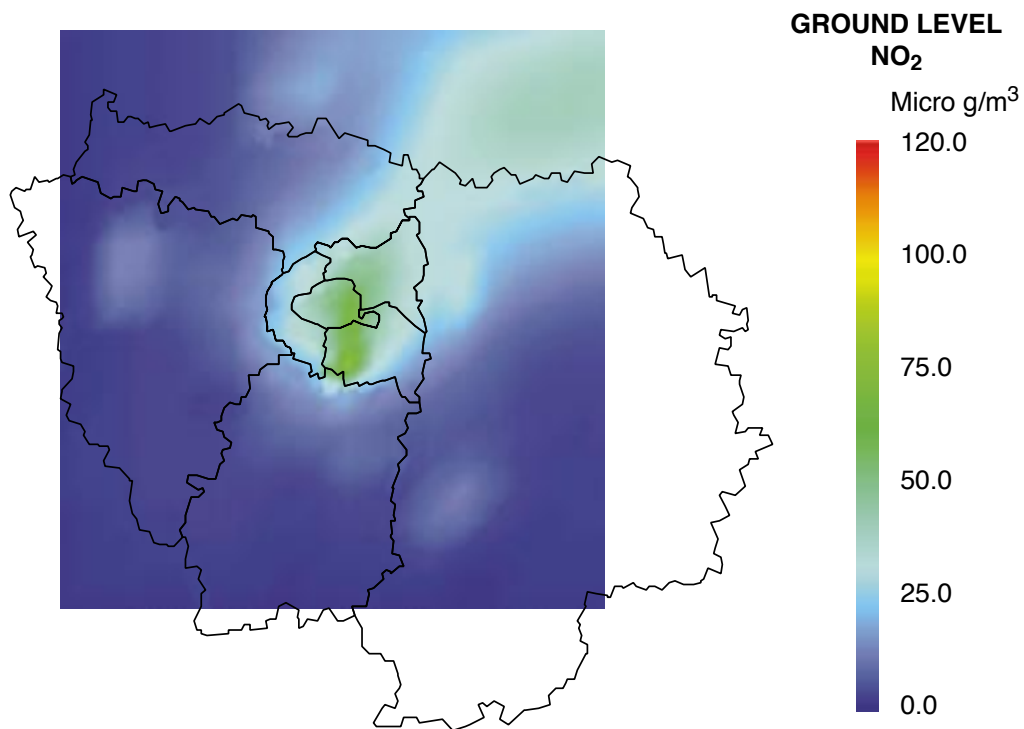

Figure 9

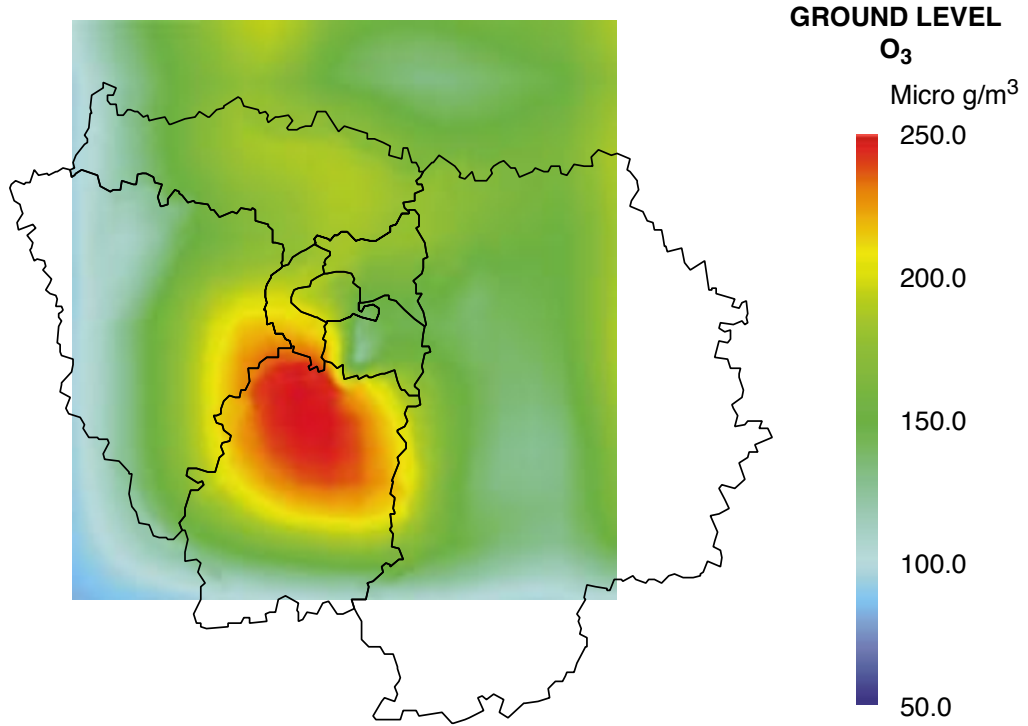NO$_2$ concentration over Paris at 15 h UTC on July 30.

Figure 10

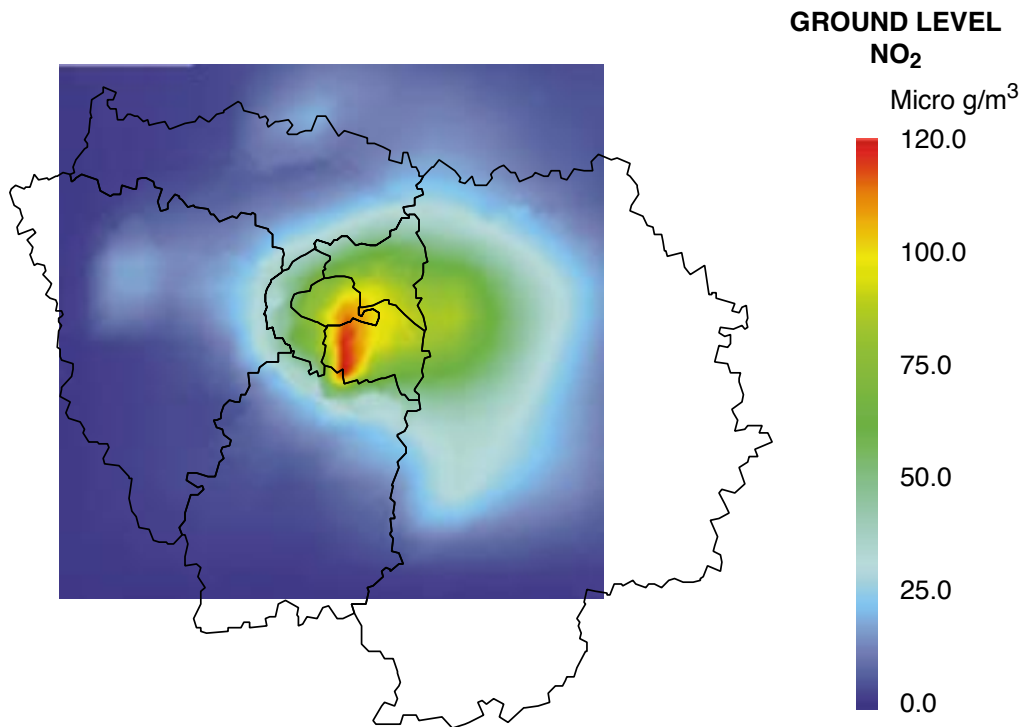O_3 concentration over Paris at 15 h UTC on July 31.

Figure 11

NO_2 concentration over Paris at 15 h UTC on July 31.

of the night and at the Saint-Jacques Tower station in late morning. Similar differences also exists at the same times for NO_2. This probably reflects the particularity of the sampling sites environment. Results are consistent since computed low values for O_3 on July 29 correspond to computed high values for NO and vice versa for the corresponding measured values.

Figures 8 to 11 show the areal distribution of O_3 and NO_2 concentrations as computed with AZUR on July 30 and 31 at 15 h UTC (5 p.m. local time). Again, results are consistent as low O_3 values are located where NO_2 values are high. Figure 8 shows that at 15 h UTC, maximum O_3 levels on July 30 (160-200 mg/m^3) are calculated 40-50 km north from the center of Paris. The July 31 episode is much more severe as O_3 concentrations are higher than 160 mg/m^3 in most locations around Paris, except in the south. This kind of map, generated avery hour, gives a very clear idea of the episode magnitude and areas actually concerned by pollution.

CONCLUSION

A numerical model of air quality at regional scale has been developed with models for meteorology, chemistry, species emission inventory, and species transport-diffusion.

It is aimed at considering the influence of different parameters related to air quality, and testing the impact of different strategies for its improvement.

The meteorological model takes into account the topography and includes a complete set of physical parameterizations in clear sky. It has been tested on boundary layer data and on mesoscale problems like land-sea breeze, orographic flows, and urban heat island.

The chemical model is detailed enough to cover a wide range of pollution scenarios with high accuracy. Its numerical performance has been optimised for vector computers. It is versatile enough to be easily customized for new conditions different from those initially taken into account.

The emission inventory model includes a fine description method of road traffic. It uses a geographic information system and can be easily adapted to different regions and different species emission conditions.

This model has been tested on a Paris summer pollution episode. Calculated results are in good agreement with ground level measurements.

Future work includes a sensitivity analysis to the different parameters to determine the relevant processes influencing air quality.

It also includes further investigations to better appreciate the influence of horizontal grid resolution on the accuracy of meteorological and atmospheric simulation results.

NOMENCLATURE

Letters

c	without index, the species concentration vector
	with one index, the corresponding species concentration
	with two indices, one species concentration value in a particular grid cell: the first index corresponds to the species concentration number and the second index corresponds to the grid cell number
D	sink term due to dry deposition of the species indicated by the index
e	turbulent kinetic energy
E	flux density of the species indicated by the first index, emitted by the vehicle type indicated by the second index
F	emission factor of the species indicated by the first index, for the vehicle type and speed indicated by the second index
F_m, F_h	Louis's functions [4] and [5]
K	air turbulent tensor (supposed diagonal)
	with one index, the corresponding air turbulent tensor diagonal term
K_{mz}	vertical turbulent coefficient for the wind
k_a	Von Karman constant (0.4)
l	mixing length in the formulation of Louis *et al.* [5]
nsp	number of chemical species
nct	number of vehicle types taken into account
R	chemical production and destruction function of the species indicated by the index
R_i	bulk Richardson number
S	source emission term of the species indicated by the index

v	without index, wind vector
	with one index, the corresponding wind vector component
V	average speed of the vehicle type indicated by the index
z_o, z_{ot}	aerodynamical and scalar roughness lengths.

Greek letters

ε	dissipation rate of turbulent kinetic energy
Φ	vehicle density of type indicated by the index
Δ*x*	cell size in the x direction
Δ*z*	cell thickness.

Indices

i	species concentration index
j	grid cell index
j+m/2	index of the grid cell interface between cell number j and cell number *j+m*
n	time step index
x, y, z	direction index.

REFERENCES

1 Elkhalfi A. and Carissimo B. (1993) Numerical simulations of a mountain wave observed during the "Pyrenees Experiment": hydrostatic/non hydrostatic comparison and time evolution. *Beitr. Phys. Atmosph.,* 66, 183-200.

2 Salles J., Janischewski J., Jaecker-Voirol A. and Martin B. (1996) Mobile source emission inventory model. Application to Paris area. *Atmos. Environ.*, 30, 1965-1975.

3 Aumont B., Jaecker-Voirol A., Martin B. and Toupance G. (1996) Tests of some reduction hypothesis made in photochemical mechanisms. *Atmos. Environ.*, 30, 2061-2077.

4 Louis J.F. (1979) A parametric model of vertical Eddy fluxes in the atmosphere. *Bound. Lay. Met.,* 17, 187-202.

5 Louis J.F., Tiedtke M. and Geleyn J.F. (1982) A short history of the PBL parametrization at ECMWF. *Proceedings, ECMWF Workshop on Planetary Boundary Layer Parametrization, Reading,* 59-80.

6 Lacis A. and Hansen J.E. (1974) A parametrization for the absorption of solar radiation in the earth's atmosphere. *J. Atmos. Sci.,* 31, 118-133.

7 Sasamori T. (1968) The radiative cooling calculation for application to general circulation experiments. *J. Appl. Met.,* 7, 721-729.

8 Stephens G.L. (1978) Radiative properties of extended water clouds. *J. Atmos. Sci.,* 19, 182-188.

9 Deardorff J.W. (1978) Efficient prediction of ground surface temperature and moisture with inclusion of a layer of vegetation. *J. Geophys. Sc.,* 63, 1889-1903.

10 Garratt J.R. (1992) *The Atmospheric Boundary Layer,* Cambridge University Press.

11 Pielke R.A. (1984) *Mesoscale Meteorological Modeling,* Academic Press Inc.

12 Stull R.B. (1988) An introduction to boundary layer meteorology. *Atmospheric Sciences Library,* Kluwer Academic Publishers.

13 Carissimo B., Dupont E. and Marchand O. (1996) Local simulations of land sea breeze cycles in Athens based on large scale operational analysis. *Atmos. Environ.* (in press).

14 Dupont E., Musson-Genon L. and Carissimo B. (1995) Simulation of the Paris Heat Island during two strong pollution events. *Air Pollution 95, Porto Carras. Proceedings (III: Urban Pollution),* ed. MM. Moussiopoulos, Power, Brebbia).

15 Carter W.P.L. (1990) A detailed mechanism for the gas-phase atmospheric reactions of organic compounds. *Atmos. Environ.,* 24A, 481.

16 Jacobson M.Z. and Turco R.P. (1994) SMVGEAR: A sparse matrix, vectorized Gear code for atmospheric models. *Atmos. Environ.,* 28A, 273-284.

17 Jacobson M.Z. (1995) A sparse matrix, computation of global photochemistry with SMVGEAR II. *Atmos. Environ.,* 29, 2541-2546.

18 MapInfo, *ADDE,* 17 rue Loise Michel, BP 29, 92301 Levallois, France.

19 Fontelle J.P., Audoux N. and Moisson F. (1992) Inventaire des émissions SO_2, NO_x, poussières, VOCNM, CH_4 dans l'atmosphère Île-de-France 1990. *Rapport CITEPA,* nov.

20 CORINAIR (1989) Working group on emission factors: environment and quality of life. *Volume 1: Methodology and Emission Factors, Final Report.*

21 Leonard B.P. and Niknafs H.S. (1990) Sharp monotonic resolution of discontinuities without clipping of narrow extrema. *Computers & Fluids,* 19.

22 Airparif, 10 rue Crillon, 75004 Paris.